Supporting Information

Spatially-Confined Electrochemical Conversion of Metal-Organic Frameworks into Metal-Sulfides and Their In-Situ Electrocatalytic Investigation Via Scanning Electrochemical Microscopy

Itamar Liberman,[a] Wenhui He,[a] Ran Shimoni,[a] Raya Ifraemov[a] and Idan Hod [*a]

Department of Chemistry and Ilse Katz Institute for nanoscale Science and Technology, Ben-Gurion University of the Negev, Beer-Sheva, 8410501, Israel.

E-mail: hodi@bgu.ac.il

Supporting information

Materials:

The chemicals: benzene-1,3,5-tricarboxylic acid (H_3BTC ≥95%), 2-methylimidazoly ($C_4H_6N_2$ ≥ 99%), thiourea (NH_2CSNH_2 ≥ 99%), lithium perchlorate ($LiClO_4$ ≥ 95%), nickel nitrate hexahydrate ($Ni(NO_3)\cdot 6H_2O$ ≥ 97%), iron chloride (FeCl3 ≥97%), terephthalic acid (BDC 98%) and ferrocene ($Fe(C_5H_5)_2$ ≥ 98%) were purchased from Sigma-Aldrich. Cobalt nitrate hexahydrate ($Co(NO_3)_2\cdot 6H_2O$ ≥ 99%) was purchased from Strem Chemicals.

The solvents: ethanol (absolute), methanol (absolute) and N,N-dimethylformamide were obtained from Bio-Lab ltd.

The Pt capillary based ultramicroelectrodes (UME) (a=5 µm, RG=10) were purchased from Bio-Logic Science Instruments.

Experimental:

FTO modified with benzene-1,3,5-tricarboxylic acid (H_3BTC): FTO slides were cleaned by sonication in detergent solution, deionized water, ethanol and acetone for 10 minutes in each solvent. After the cleaning process was finished, the FTO slides were dried in air. Two clean FTO slides were placed next to each other with their conductive

sides pointing outward and immersed into 20 ml of 5 mM H_3BTC solution in methanol for 12 hours. Afterwards, the FTO slides were washed gently with methanol and dried in air.

ZIF-67 thin film growth on FTO modified with H_3BTC: 10 ml methanol with 2-methylimidazole (40 mM) and 10ml methanol containing $Co(NO_3)_2$ (20 mM) were mixed together. Two FTO slides modified with H_3BTC were placed next to each other with the conductive sides pointing outward and dipped into the solution for at least 8 hours. After this period the two FTO slides were transferred into freshly mixed solution. This process was repeated 8 times to form a homogeneous and strongly attached layer ZIF-67 over the conductive sides of the FTO slides (FTO-ZIF-67).

Bimetallic (Fe,Ni)-MIL-53 synthesis: The (Fe,Ni)-MIL-53 was synthesis via previously reported synthesis[1]. In general, BDC (66.4 mg) was dissolved in 28 ml of DMA by ultrasonication. Latter, 279.6 mg of $Ni(NO_3)\cdot 6H_2O$ and 64.9 mg of $FeCl_3$ were mix in 20ml of DMA. The two mixers were combined and stirred for two minutes than divided in to four Teflon vials (about 12 ml each). The vials were place in stainless steel autoclaves and heated in oven at 150 °C for 3 h. The products were collected by centrifugation and washed three times by ethanol three times with water and three times more with ethanol. The clean product was dried in vacuum oven over night. The crystal structure was confirmed by XRD (see figure S12) by comparing its spectra to previous reports[1].

Electrophoretic Deposition (EPD) of (Fe,Ni)-MIL-53 on FTO slides: FTO slides were clean by sonication in detergent solution, deionized water, ethanol and acetone for 10 minutes in each solvent. 50 mg of (Fe,Ni)-MIL-53 powder was dispersed in 50 mL of DMF with 700 µl of water and 5 mg of $Ni(NO_3)\cdot 6H_2O$. A thin layer of (Fe,Ni)-MIL-53 was coated over a clean FTO slides in this solution, by applying potential bias of 10 V between two FTO slides, 0.7 cm apart (conductive side inward), for 2 min cycles using ENDUROTM high-voltage DC suppler. This procedure was reaped 2 more times up until homogeneous layer of (Fe,Ni)-MIL-53 was deposited over the negatively charged FTO electrode (FTO-(Fe,Ni)-MIL-53). The electrode was than lifted out of the solution and dry in oven at 120 °C for 2 h.

Electrochemical conversion of ZIF-67 in to CoS_x in a localized fashion: FTO-ZIF-67 electrode was placed inside the compartment in the custom-made electrochemical cell designed to work in Biologic SECM-150 setup (figure S2). Pt wire was used as counter and reference electrodes and Pt ultramicroelectrode (a=5 µm, RG=10) was used as a working electrode. 800 µl of DMF solution containing ferrocene (5mM) and lithium perchlorate (0.2 M) was introduced to the cell. The tip-to-substrate distance (d_{T-S}) was confirmed by an approach curve experiment in this solution by holding the tip potential constant at 0.7 V (vs Pt wire) and approaching the surface at 2 µm/sec. The recorded tip current and the distance were fit to the theoretical model by MIRA SECM simulation software. Then we added 1ml of DMF containing 1 M thiourea and 200 µl of ultrapure water (18.2 MΩ·cm) to this solution and placed the SECM tip 11.5 ±0.5 µm above the FTO-ZIF-67 surface. In order to generate a localized flux of OH^- at the tip, we scanned the tip voltage from -0.1 V to -1.5 V (vs Pt wire) by cyclic voltammetry (0.5 V/sec) 100 times (1 EC-MOF cycle). After this process we moved the tip 20 µm up and back to the same location in order to mix the solution gently. We repeated this conversion cycle 30 (30X), 60 (60X), 90 (90X) times and 30 times over 3 close locations (3X30X) to produce different conversion rates and patterns. After those conversion processes the FTO-ZIF-67 electrode was carefully washed with water and ethanol and dried in air. The dry samples were characterized by several methods.

Localized Electrochemical conversion of (Fe,Ni)-MIL-53 in to $NiFeS_x$: The FTO-(Fe,Ni)-MIL-53 electrode was placed in the same system described above. 1 ml of DMF solution containing ferrocene (5mM) and lithium perchlorate (0.2 M) was introduced to the cell. The tip-to-substrate distance (d_{T-S}) was confirmed by an approach curve experiment in this solution by holding the tip potential constant at 0.7 V (vs Pt wire) and approaching the surface at 2 µm/sec. Then we added 1ml of DMF/ ultrapure water (50:50 %v) solution, containing 1 M of thiourea to the cell and place the SECM tip 12 ±0.5 µm above the FTO-(Fe,Ni)-MIL-53 surface. The tip voltage was scanned from 0.1 V to -1.3 v (vs Pt wire) by cyclic voltammetry (0.5 V/sec) 100 times (1 EC-MOF cycle). After this process we moved the tip 20 µm up and back to the same location in order to mix the solution gently. We repeated this conversion cycle 60 times. The FTO-

(Fe,Ni)-MIL-53 was then washed with water and ethanol and dried in air. The sample was then characterized be SEM and EDS.

Hydrogen evolution reaction (HER) activity mapping: A ZIF-67, 60 conversion cycles sample was prepared as we described above. The cell was washed up with new solution by carefully taking out the conversion solution and addition of 2ml of 0.1M lithium perchlorate solution in ultrapure water/DMF (20% v/v). The washing was repeated 3 times in order to remove any remaining of the conversion solution. The SECM tip was placed 11.5 µm above the surface of the electrode. The FTO-ZIF-67 electrode conductive side was connected to the SECM potentiostat. The HER mapping was done in this solution by holding the surface potential at -1 V (vs NHE), sufficient to reduce the water in the solution and to produce hydrogen gas, and holding the tip potential at 1V (vs NHE) that is sufficient to oxidize back the surface product (H_2). The surface scan rate was 30 µm/sec with 10 µm intervals in the Y axis. The collected data was edited with MIRA SECM simulation software to reduce the surface tilt influences. All potentials in this section are reported versus NHE by first converting the potential versus $Fc\backslash Fc^+$ (CV at 50 mV/s vs Ag/AgCl) and then converting to NHE by literature values[2] ($E_{NHE} = E_{Ag/AgCl} + 0.63 - E_{Fc/Fc+}$ (vs Ag/AgCl)).

Oxygen evolution reaction (OER) activity detection over $FeNiS_x$ converted pattern: A (Fe,Ni)-MIL-53 60 conversion cycles sample was prepared as described above. The solution was then washed three times using a fresh solution containing ultrapure water/DMF (20% v/v) and 0.1 M of lithium perchlorate as electrolyte. The SECM tip was then place 12 µm above the electrode surface. The OER activity detection by substrate-generation tip-collection (SG-TC) mode of the SECM. The substrate potential was linearly scanned from 1V to 2V (vs NHE) in order to oxidize water to O_2 while the tip potential was held at -0.9V (vs NHE) to effectively reduce the substrate-produced O_2. The potentials in this section are reported versus NHE by first converting the potential versus $Fc\backslash Fc^+$ (CV at 50 mV/s vs Ag/AgCl) and then converting to NHE by literature values[2] ($E_{NHE} = E_{Ag/AgCl} + 0.63 - E_{Fc/Fc+}$ (vs Ag/AgCl)). (an Ag/AgCl reference electrode was originally used in this section).

Physical methods: The crystalline structure of the FTO-ZIF-67 electrode was confirmed by X-ray diffraction (XRD) measured with PANalytical's Empyream multi-

purpose diffractometer instrument and Cu-Kα (0.15405 nm) radiation. Scanning electron microscope (SEM) images were taking with Verios XHR 460L SEM operating at 2 kV accelerating voltage. EDS point and mapping also done in this instrument with INCA 400 Oxford EDS analyzer. Raman spectra and mapping were done in Horiba LabRam HR evolution micro-Raman system, equipped with a Synapse Open Electrode CCD detector air-cooled to -60 °C. The excitation source was a 532 nm laser with a power on the sample of 0.5 mW. The laser was focused with an x50 objective to a spot of about 1 µm. The measurements were taken with a 600 g mm^{-1} grating and a 100 µm confocal microscope hole. Typical exposure time was 30 seconds. The X-ray photoelectron spectroscopy (XPS) data were collected using an X-ray photoelectron spectrometer ESCALAB 250 ultrahigh vacuum ($1*10^{-9}$ bar) apparatus with an AlK^{α} X-ray source and a monochromator. To characterize the formed micron-sized CoS_x pattern, a localized X-ray beam size of 80 µm was used. Survey spectra was recorded with pass energy (PE) 150 eV and high energy resolution spectra were recorded with pass energy (PE) 20 eV. To correct charging effects, all spectra were calibrated relative to a C 1s peak position at 284.8 eV. Processing of the XPS raw data was done with AVANTGE program.

Supplementary Results:

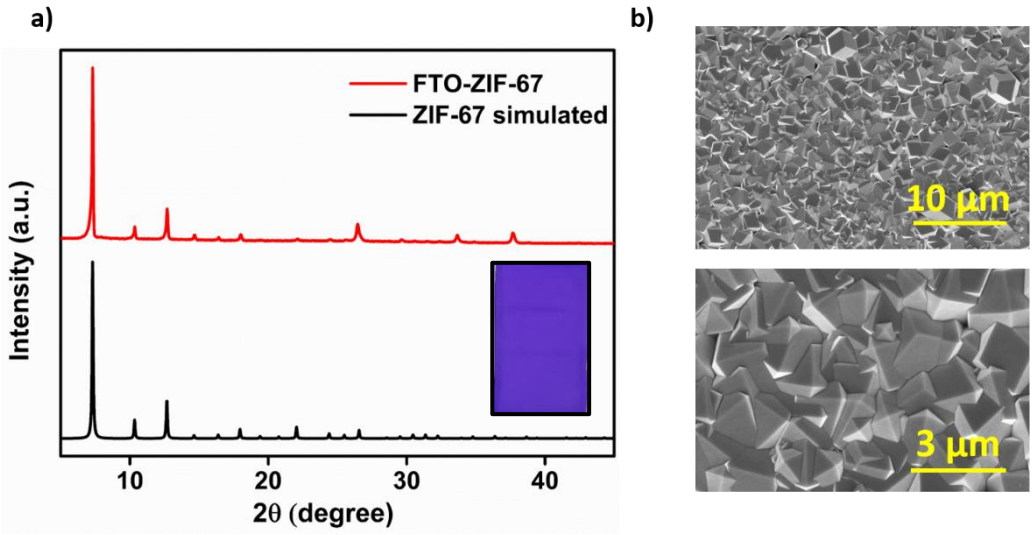

Figure S1: a) XRD spectra of the FTO-ZIF-67 electrode (red) and ZIF-67 simulated spectra (black) and photo of the as prepared FTO-ZIF-67. b) SEM images of the ZIF-67 MOF over the FTO electrode

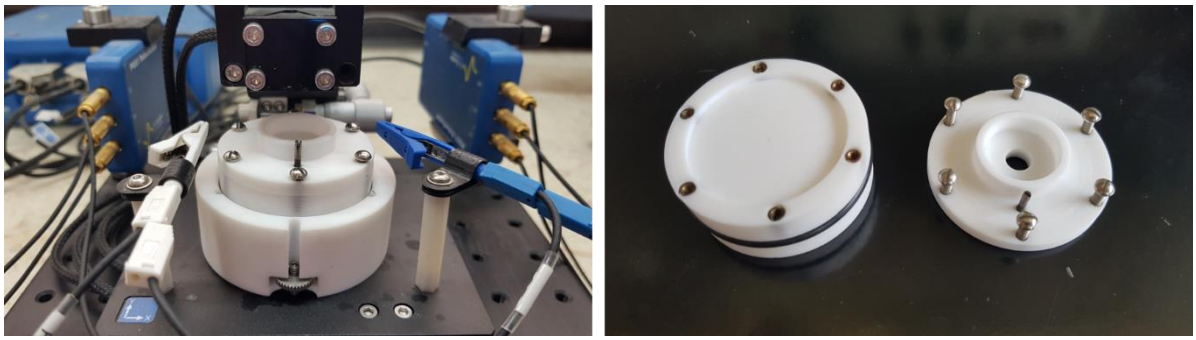

Figure S2: Photos of the custom made electrochemical cell designed to work with a bio-logic SECM-150 instrument

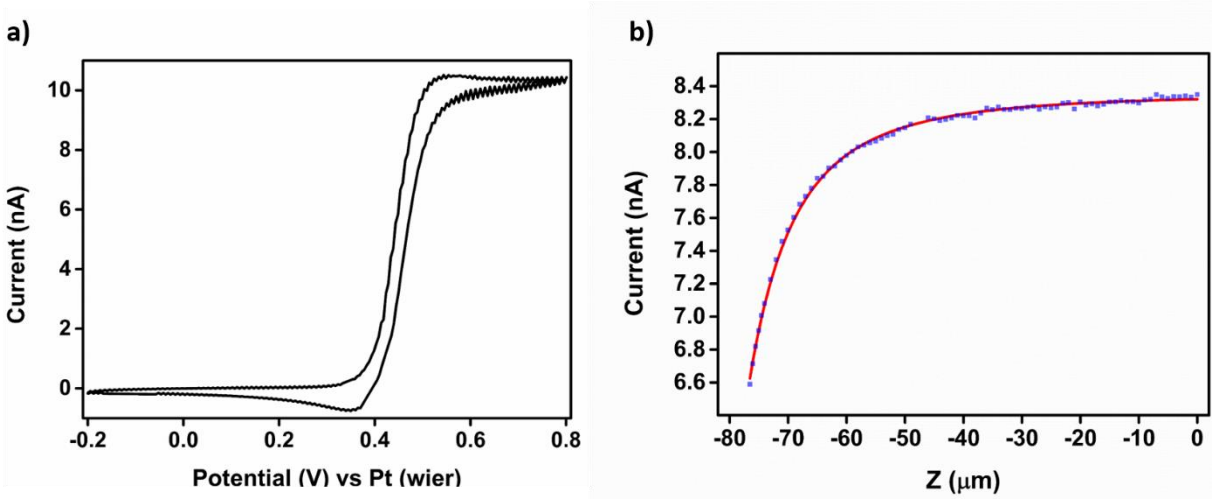

Figure S3: a) Typical CV scan (-0.2 to 0.8V vs Pt wire 0.5V/sec) at the SECM UME tip in DMF solution containing ferrocene (5mM) and lithium perchlorate (0.2M) a steady-state current can be seen at 0.7V (vs Pt wire). b) Typical SECM negative feedback approach curve to the FTO-ZIF-67 electrode surface. The recorded tip current as a function of the distance (blue square) and the it fit to the theoretical model (red).

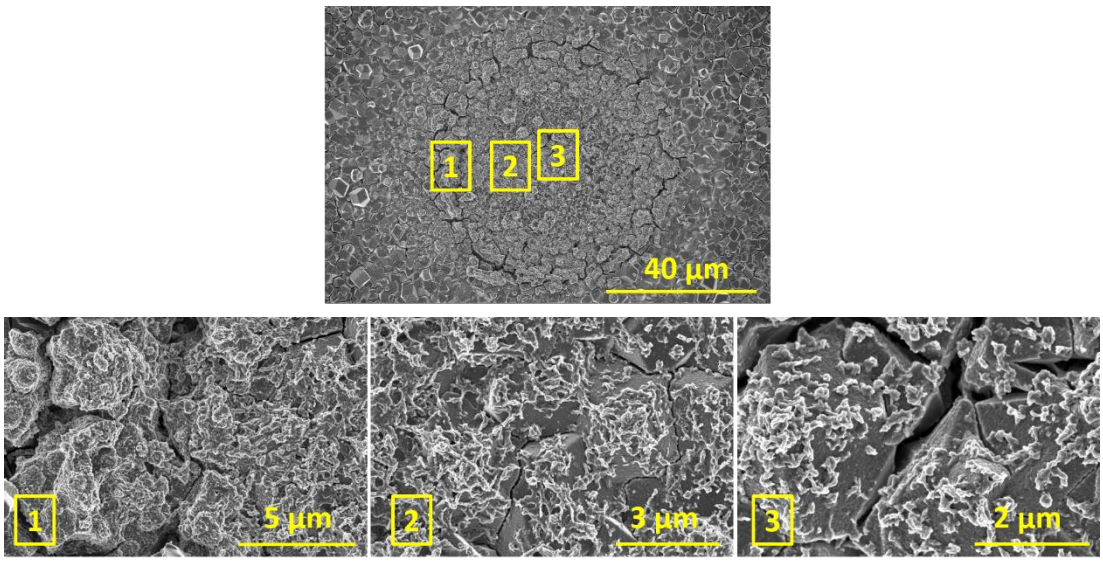

Figure S4: SEM images of 30X full conversion pattern image (top) and high magnification images for different areas in the converted pattern as marked by numbers (bottom), with high conversion rate to low conversion rate going from left to right (or from the ring to the center).

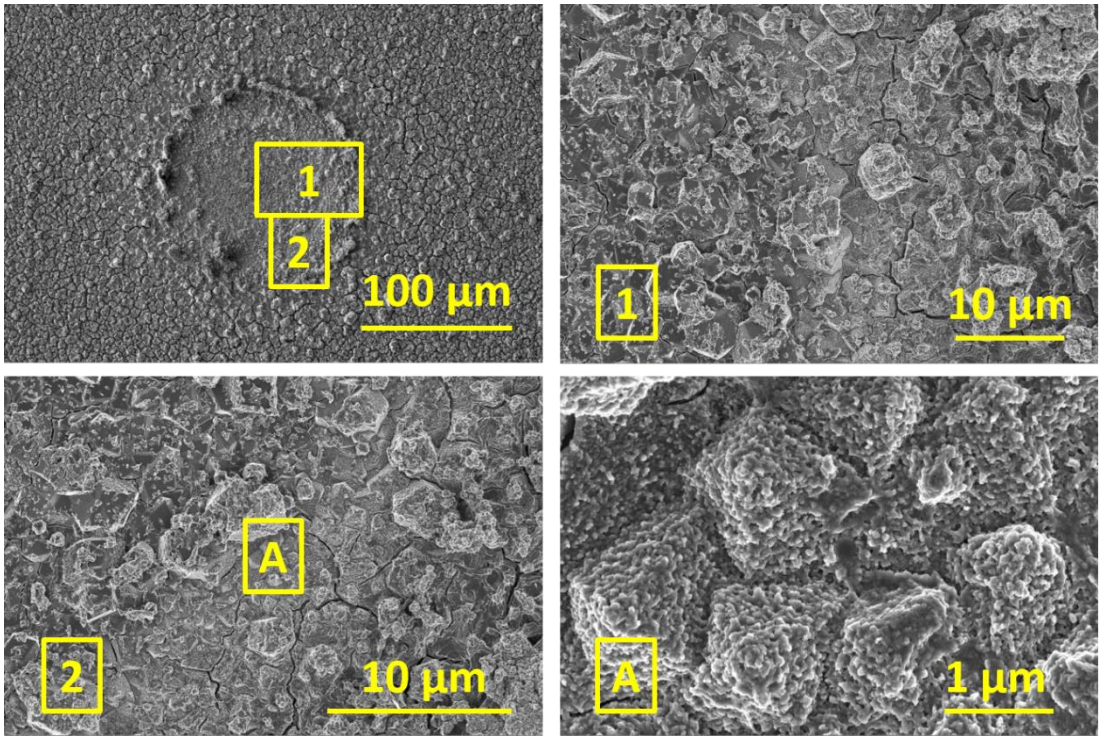

Figure S5: SEM images of 60X full conversion pattern image (top left) and high magnification image for different areas in the converted pattern as marked by numbers and letters (top right and bottom). A gradual conversion rate can be seen in numbers 1 and 2 going from left to right, and top left to bottom right, respectively (center to ring). A is a magnified image of the marked location in image 2 showing the change in the ZIF-67 morphology while it preservies its shape.

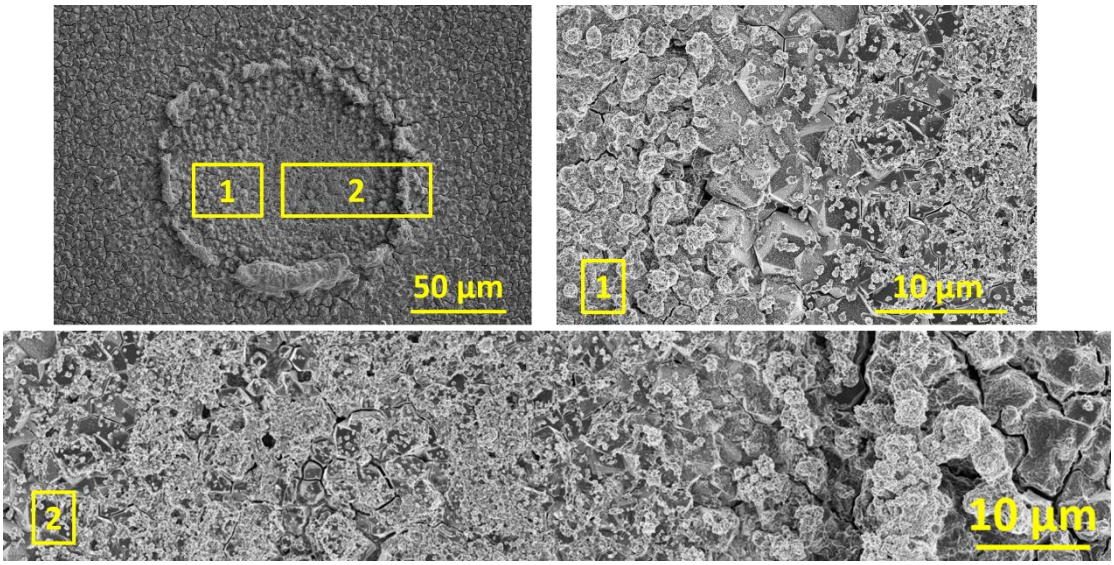

Figure S6: SEM images of 90X full conversion pattern image (top left) and high magnification image for different areas in the converted pattern as marked by numbers (top right and bottom), showing a gradual conversion rate going from the center outward (right to left in 1 and left to right in 2)

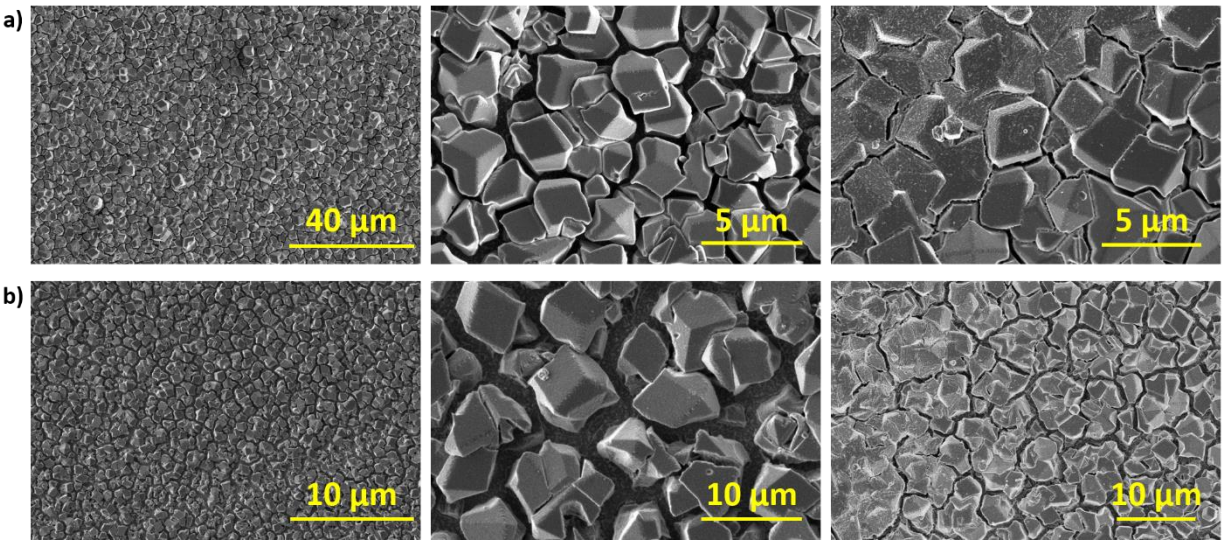

Figure S7: a) SEM images of the converted pattern's (30X) surrounding area, the two in the left are far from the conversion pattern and the one in the right is close to it. b) SEM images of the converted pattern's (90X) surrounding area, the two in the left are far from the conversion pattern and the one in the right is close to it.

a)

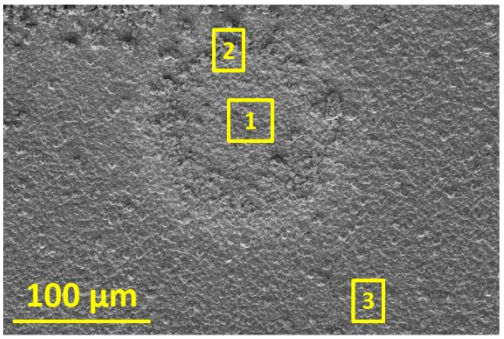

	O Atom %	S Atom %	Co Atom %	S:Co ratio
1	8.7	0.2	8.2	1:41
2	40.3	2.2	12.9	1:5.86
3	13.7	0.2	6.9	1:34.5

b)

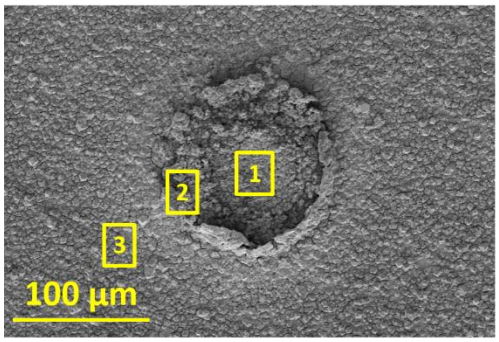

	O Atom %	S Atom %	Co Atom %	S:Co ratio
1	18.5	0.7	9.7	1:13.85
2	45.9	4.3	18.3	1:4.25
3	21.2	0.6	8.0	1:13.33

c)

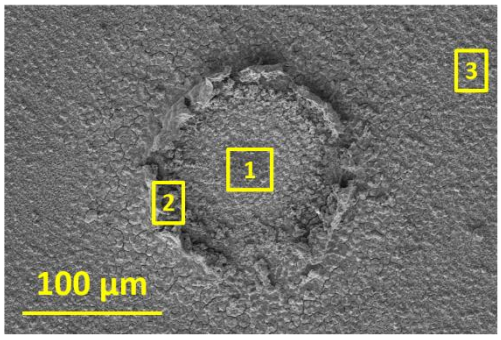

	O Atom %	S Atom %	Co Atom %	S:Co ratio
1	8.0	0.3	9.0	1:30
2	33.1	2.0	7.5	1:3.75
3	29.1	0.9	8.3	1:9.2

Figure S8: EDS point measurements and the atomic percentages of the selected elements at different locations in the converted pattern for a) 30X. b) 60X. c) 90X.

a)

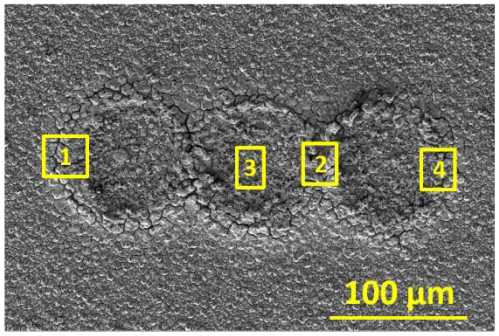

	O Atom %	S Atom %	Co Atom %	S:Co ratio
1	49.8	4.3	22.6	1:5.3
2	53.6	4.2	22.8	1:5.4
3	16.0	2.0	14.8	1:7.4
4	53.7	5.2	22.5	1:4.3

b)

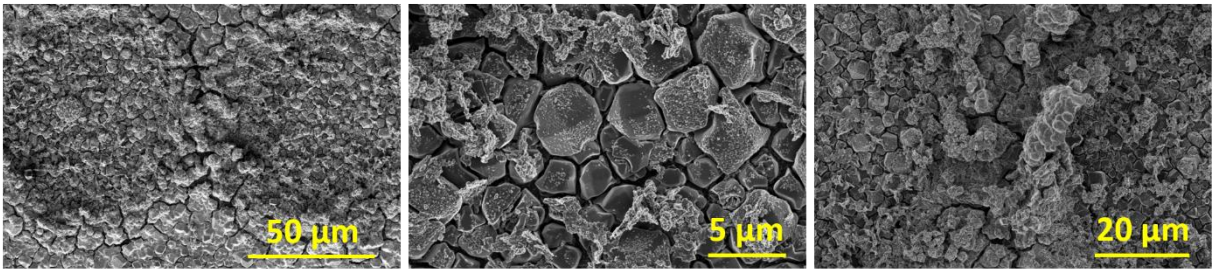

Figure S9: SEM image (left) and EDS measurements (right table) at the mark locations for the 3X30X sample. b) SEM high magnification image of different locations at the 3X30X conversion pattern

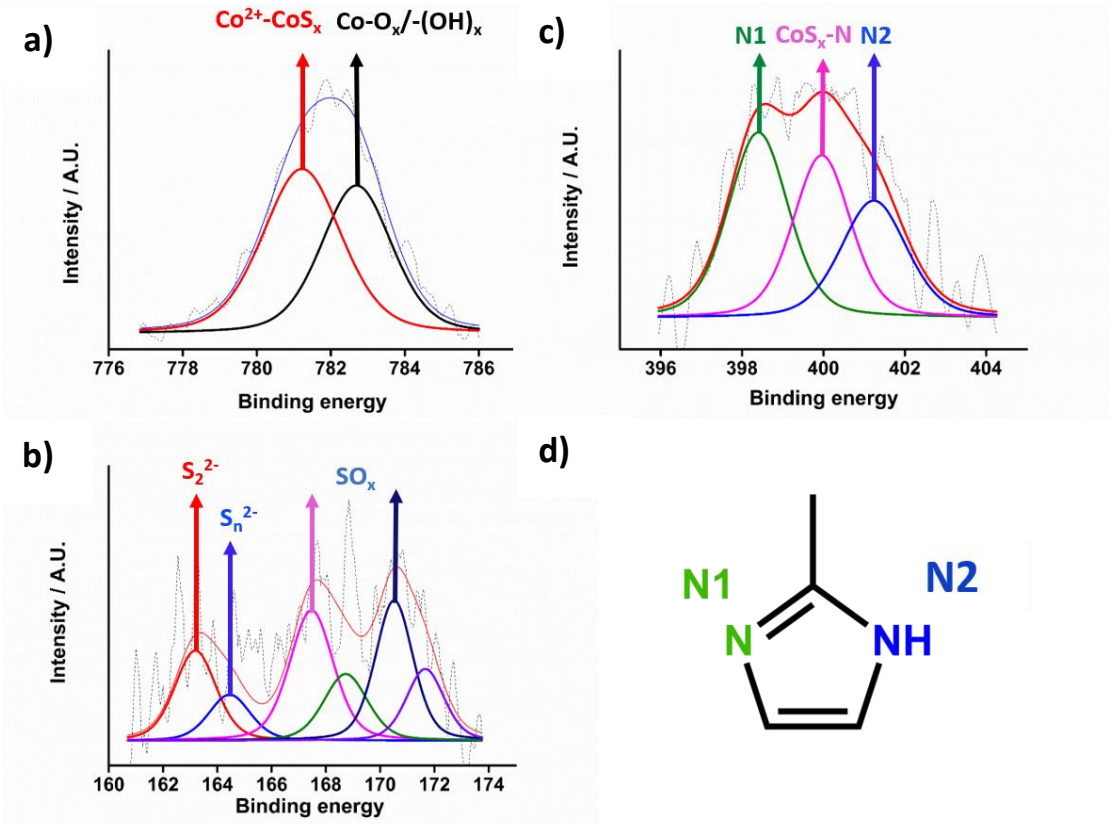

Figure S10: XPS measurement over the CoS_x 60X conversion pattern: a) $Co2p^{3/2}$ biding energy (BE) showing two clear peaks at 781.2 eV and 782.7 eV correlated to the biding energy of Co^{2+}-CoS_x and CoS_x-O_x/-$(OH)_x$ respectively, in good agreement with previous reports[3-5]. b) S2p BE spectrum showing two peaks at 163.2 and 164.5 eV which are corelated to S_2^{2-} and polysulfides (S_n^{2-} n>2) species respectively[5-8] as previously reported and two peaks at 167.47 and 170.5 eV (and there satellite peaks) corresponding to SO_x species (SO_4^{2-} and SO_3^{2-}) that formed due to oxidation of the sample[1, 5]. c) N1s BE spectra show three peaks at 398.4, 401.2 and 399.9 (eV) which are correlated to the free 2-mathel imidazole nitrogen and a nitrogen bound to a CoS_x species respectively[5]. d) Schematic representation of the different chemical modes of nitrogen in our system.

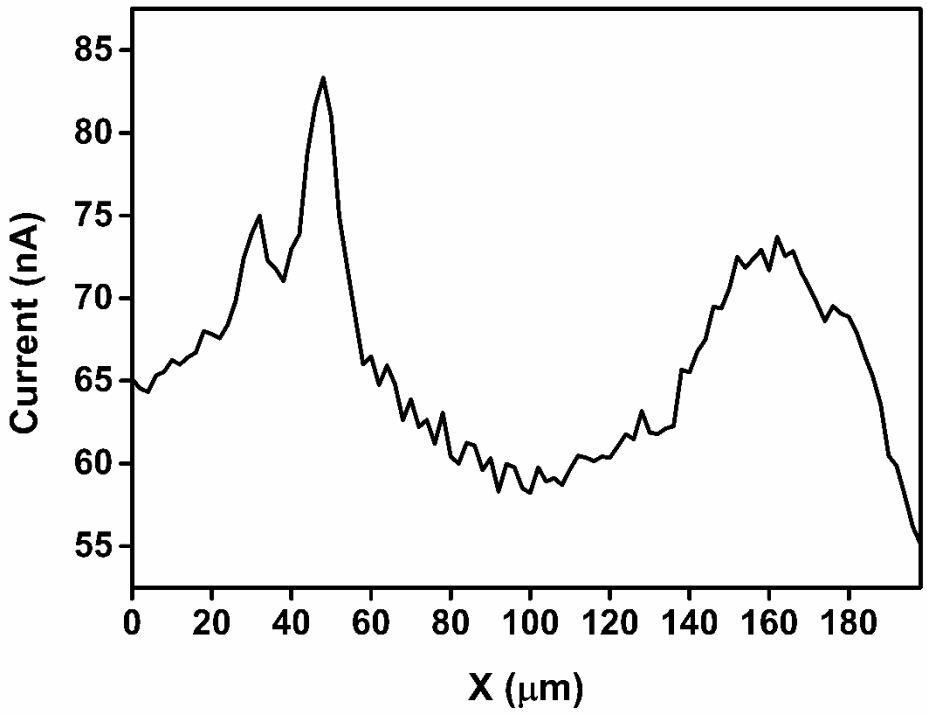

Figure S11: HER activity line scan of the 60X converted CoS_x pattern. The tip potential was held at 1 V (vs NHE) while the substrate potential was -1 V (vs NHE). The tip electrode was scanned in the X-axis at a rate of 30 μm/sec.

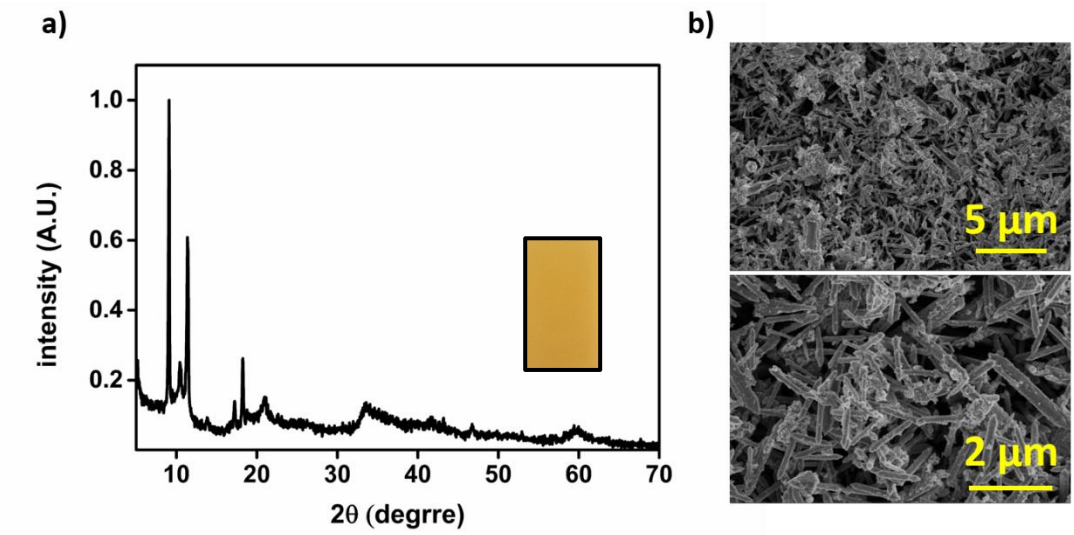

Figure S12: a) XRD spectra of the (Fe,Ni)-MIL-53 powder. The inset shows an optical image of the as-prepared FTO-(Fe,Ni)-MIL-53 electrode. b) SEM images of the FTO-(Fe,Ni)-MIL-53 electrode.

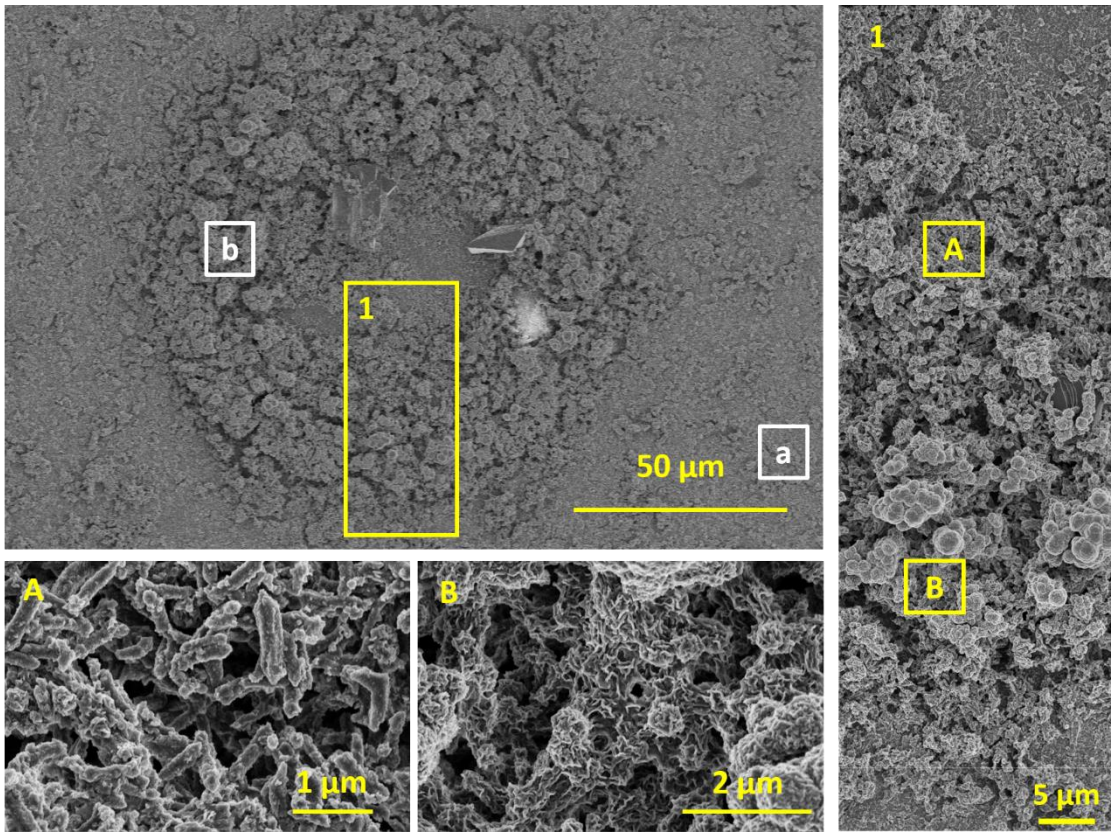

Figure S13: SEM image of the full (Fe,Ni)-MIL-53, 60 cycles conversion pattern (top left) and high magnification images at the marked locations (A, B in yellow rectangular area 1) showing the gradual conversion rate going from the center outward. In addition, white rectangular areas (a, and b) mark the spots for EDS measurments in Table S1 below.

	Ni+Fe:S
a	14.4:1
b	8.80:1

Table S1: results of EDS at the mark locations in figure S13 (a, b) comparing the molar ratio between Ni+Fe and S, showing a significantly higher S content at the converted area.

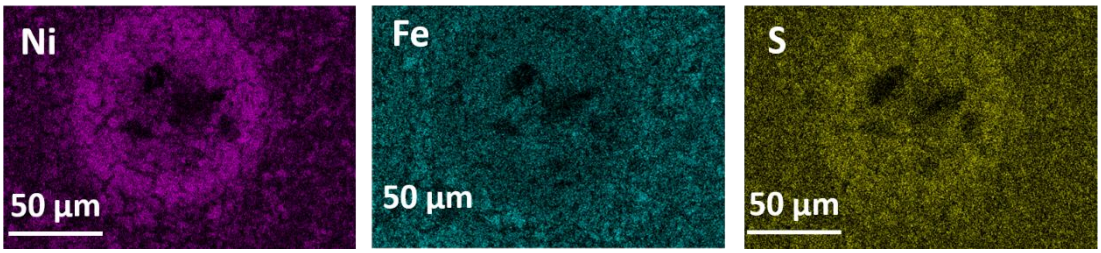

Figure S14: EDS elemental mapping of the 60 cycles (Fe,Ni)-MIL-53 conversion pattern for S (yellow) Fe (turquoise) and Ni (purple).

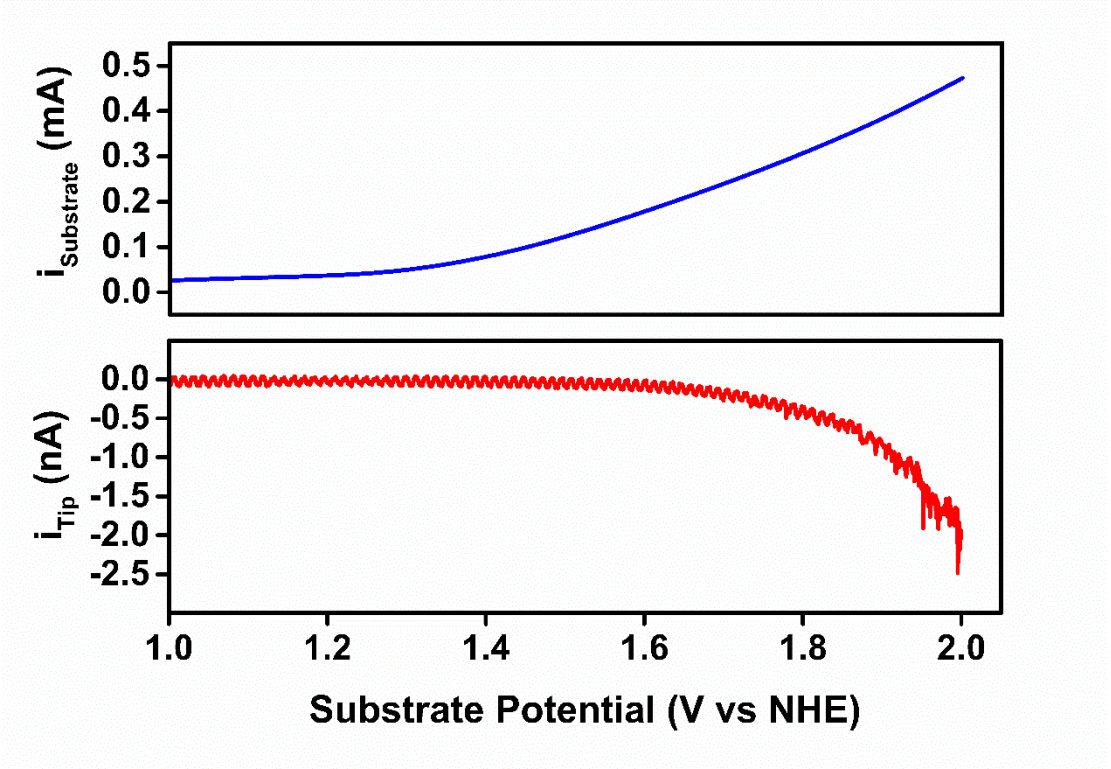

Figure S15: SG-TC measurement over the (Fe,Ni)-MIL-53, 60 cycles conversion pattern. The SECM tip potential was held at -0.9 V (vs NHE) and the substrate's potential was linearly scanned from 1 V to 2 V (vs NHE). The substrate current vs potential in the top graph (blue) and the tip current vs surface potential in the bottom graph (red).

References:

1. W. He, H.-M. Gao, R. Shimoni, Z.-Y. Lu and I. Hod, *ACS Appl. Energy Mater.*, 2019, **2**, 2138-2148.
2. V. V. Pavlishchuk and A. W. Addison, *Inorg. Chim. Acta*, 2000, **298**, 97-102.
3. S. Dou, L. Tao, J. Huo, S. Wang and L. Dai, *Energy Environ. Sci.*, 2016, **9**, 1320-1326.
4. T. Yoon and K. S. Kim, *Adv. Funct. Mater.*, 2016, **26**, 7386-7393.
5. W. He, R. Ifraemov, A. Raslin and I. Hod, *Adv Funct Mater*, 2018, **28**, 1707244.
6. Y. Chen, P. D. Tran, P. Boix, Y. Ren, S. Y. Chiam, Z. Li, K. Fu, L. H. Wong and J. Barber, *ACS nano*, 2015, **9**, 3829-3836.
7. X. Ge, L. Chen, L. Zhang, Y. Wen, A. Hirata and M. Chen, *Adv. Mater.*, 2014, **26**, 3100-3104.
8. Y. H. Chang, C. T. Lin, T. Y. Chen, C. L. Hsu, Y. H. Lee, W. Zhang, K. H. Wei and L. J. Li, *Adv. Mater.*, 2013, **25**, 756-760.